Comparison of the performance of latent heat flux products over southern hemisphere forest ecosystems: estimating latent heat flux error structure using in situ measurements and the triple collocation method

Verónica Barraza Bernadas, Francisco Grings, Natalia Restrepo-Coupe & Alfredo Huete

Published online: 03 Apr 2018.

Submit your article to this journal ⤤

View related articles ⤤

View Crossmark data ⤤

Taylor & Francis
Taylor & Francis Group

Check for updates

Comparison of the performance of latent heat flux products over southern hemisphere forest ecosystems: estimating latent heat flux error structure using *in situ* measurements and the triple collocation method

Verónica Barraza Bernadas[a], Francisco Grings[a], Natalia Restrepo-Coupe[b,c] and Alfredo Huete[b]

[a]Institute of Astronomy and Space Physics (IAFE-CONICET-UBA), CABA, Buenos Aires, Argentina; [b]Plant Functional Biology and Climate Change Cluster, University of Technology Sydney, Sydney, Australia; [c]Department of Ecology and Evolutionary Biology, University of Arizona, Tucson, AZ, USA

ABSTRACT

In this study, we compared different remote-sensing (RS)-based land surface models (LSM) and reanalysis latent heat flux (LE) products over different forest ecosystems. We analysed the performance of three RS products, the MOD16A2, the Breathing Earth System Simulator (BESS) model, and a combined optical-microwave model (COM) in their ability to replicate eddy covariance (EC) flux observations of LE at eight southern hemisphere forest ecosystems and compared their results to simulated LE from the offline LSM (GLDAS/NOAH) and a reanalysis LE dataset (MERRA). To determine spatial uncertainties, we used the triple collocation (TC) method, which does not require *a priori* knowledge of the true LE value, at selected Australian EC locations and over an area without *in situ* measurement (the Dry Chaco Forest (DCF), Argentina). The spatial pattern of the TC results was commensurable with uncertainties calculated using EC observations, indicating that the TC method is a robust technique to estimate spatial uncertainties. As global products have been validated with EC measurement from Ozflux stations, we hypothesized and found, using the TC model, that LE products achieve a better performance over areas with EC from networks than over sites without ground-based measurements and may reflect over-calibration of models or a need for a more diverse representation of ecosystems at flux tower networks.

1. Introduction

To determine present and future water, energy, and carbon fluxes it is essential to understand the different ecosystem responses to meteorology and climate. One of the most important component of the energy budget is evapotranspiration (ET) and its energy equivalent the latent heat flux (LE), since ET (or LE) uses more than half of the

CONTACT Verónica Barraza Bernadas ✉ vbarraza@iafe.uba.ar 🖂 Buenos Aires, ArgentinaInstitute of Astronomy and Space Physics (IAFE-CONICET-UBA), CABA
➕ Supplemental data for this article can be accessed here.

total solar energy absorbed by land surfaces (Trenberth, Fasullo, and Kiehl 2009). The eddy covariance (EC) technique (Baldocchi, Hincks, and Meyers 1988) provides a tool to estimate *in situ* ET at high temporal resolution necessary to examine processes, but also at much greater spatial scales than other direct method (e.g. sap flow). However, limited networks of EC towers globally limit quantification of ET across large areas. In special, there are few (or none) EC towers over different Australian Savannas and South American forests compared to their northern hemisphere contra parts.

Remote sensing (RS) is considered one of the most viable method for producing spatially distributed global or regional ET products. Various methods have been developed using RS observations to estimate ET and LE at regional scale. Among these models, the official Moderate Resolution Imaging Spectroradiometer (MODIS) ET product (MOD16) drives the Penman-Monteith (PM) equation (Allen et al. 1998; Monteith 1985) with daily meteorological reanalysis data and 8-day remotely sensed vegetation property dynamics (MOD15 leaf area index (LAI) product). Another RS product is the Breathing Earth System Simulator (BESS), which is a concise process-based model used to estimate carbon and water fluxes at global scale that used a range of data streams in MODIS atmospheric and land products with ancillary data (Jiang and Ryu 2016). These two global products have been validated with EC measurements from Ameriflux stations (Mu et al. 2007; Mu, Zhao, and Running 2011) and from FLUXNET network sites (Jiang and Ryu 2016). A recently developed algorithm estimates surface conductance (G_s) using passive microwave and optical indices (combined optical-microwave model (COM)) in dense forest areas (Barraza et al. 2015) improving LE schemes that relied on a single satellite product. An extended analysis in Savannas evaluated the performance of the COM model replacing local meteorological with global meteorological data (Barraza et al. 2017).

LE (and ET) at global to regional scales can also be simulated using land surface models (LSMs). The Global Land Data Assimilation System (GLDAS) (Rodell et al. 2004) provides a series of land surface states (e.g. soil moisture and surface temperature) and fluxes (e.g. evaporation, land heat flux products) simulated by four LSMs (Community Land Model, Mosaic, Noah, and The Variable Infiltration Capacity) (Rosero et al. 2009; Ek 2003; Rodell et al. 2004). The most relevant limitation of LSMs is that their strong theoretical framework can lead to greater uncertainty than RS methods, due to a multitude of data types used as input (RS, re-analysis, etc.) (Rosero et al. 2009).

The goal of RS and LSM products (Mu et al. 2007; Barraza et al. 2015; Rodell et al. 2004) is to estimate LE over areas without *in situ* measurements. Since global product was validated over regions with a relatively good measurement network (e.g. Fluxnet EC locations) (Mu et al. 2007), lower errors are expected to be found over this areas compared to other ecosystems and locations non-represented at the EC network (e.g. South America). To address the uncertainties at locations missing ground observations, an alternative validation technique called the triple colocation (TC) method has been proposed by Stoffelen (1998). The TC has been used to evaluate the soil moisture (Yilmaz and Crow 2014), LAI (Fang et al. 2012), and other products, over areas without *in situ* measurements. The TC method requires three uncorrelated estimates as to rank the different products' uncertainties without any *a priori* knowledge of the true value of interest or input variables.

In this study, we evaluated and compared the performance of LE estimates over Southern Hemisphere Forest ecosystem with (1) *in situ* and (2) without ground-based measurements. We used three RS, one LSM, and one reanalysis LE products. We tested the hypothesis that LE products offer a better performance over areas with available EC datasets than over sites without *in situ* flux measurements. Our objectives were: (1) to estimate uncertainties of four LE products over contrasting areas using the TC model, and (2) to compare the performance of the different LE models over EC forest sites using *in situ* measurements and the TC method at ecosystems with EC observations.

2. Methodology

2.1. *Study area*

We divided the forest areas in two types: (1) areas with and (2) without ground LE measurements. We analysed four EC forests ecosystems (Savannas) and one forest site without *in situ* measurements (Dry Forest). We selected these sites because both Savannas and dry forests are complex ecosystems with multilayer structures. The EC sites (1) were: Howard Spring (12.48° S, 131.15° E), Adelaide Rivers (13.09° S, 131.12° E), Daly River (14.16° S, 131.84° E), and Dry River (15.25° S, 132.37° E) (Table 1 and Figure 1). These EC sites are located across the North of the Australia along a rainfall gradient of 1100 km in length known as the North Australian Tropical Transect (NATT) (Koch et al. 1995). The vegetation from north to south is dominated by *Eucalyptus woodlands, tropical Eucalyptus woodlands*, and *Eucalyptus open forests*. The EC observations obtained from these sites included half-hour measurements of LE and meteorological variables. The data were assessed for quality and gap-filled using techniques described by Restrepo-Coupe et al. (2015).

We selected a deciduous dry forest located in the Dry Chaco region (DCF) without EC (2), the semiarid and arid Chaco region because: (1) its homogeneity, (2) the availability of *in situ* meteorological measurements (e.g. precipitation and temperature), and (3) access to passive microwave signatures characterized by low spatial resolution and LE fluxes from the correspondent COM model. The selected area is part of the extensive 'Gran Chaco Forest' dry forest, one of the largest remaining tracts of Savannas in the world and the second largest forested ecosystem outside the Amazon in South America (Gasparri and Baldi 2013). The DCF covers an area of 176,000 km^2 and includes a significant fraction of the largest continuum of woodlands in Argentina, locally called 'El Impenetrable'. The vegetation is dominated by dry forest trees and shrubs; scatter natural grasslands occur in areas with sandy soils and frequent fires and recently deforested plots are now used for soybean cultivation (Gasparri and Grau 2009).

Table 1. Description of eddy covariance flux tower forest locations used in this study. Sites are described by their canopy height (h), measurement height (z), years of available eddy covariance data (Years), latitude (Lat), longitude (Lon).

Code	Name	Lat (°)	Lon (°)	h (m)	z (m)	Years	Reference
AU-Hsp	Howard Springs	12.48	131.15	18.9	23	2001–11	Hutley et al. (2011)
AU-Ade	Adelaire Rivers	13.09	131.12	12.5	15	2007–09	Sea et al. (2011)
AU-DaS	Daly River	14.16	131.84	16.4	23	2007–11	Hutley et al. (2011)
AU-Dry	Dry River	15.26	132.37	12.3	15	2010–11	Sea et al. (2011)

2.2. *Latent heat flux*

In this study, we took the ET (and its energy equivalent, LE) product of three distinctly conceptual models (RS, LSM, and reanalysis, Table 2). Two of the RS-derived LE calculations are based on the Penman-Monteith equation, the regional COM model (Barraza et al. 2017), and the global MOD16A2 product (Mu et al. 2007); however, these two models differ in their inputs (satellite-derived datasets) and in the method used to estimate vegetation contribution to ET (represented by the surface conductance). Opposite to the two RS models, the BESS product (Jiang and Ryu 2016) couples algorithms that compute atmospheric radiative transfer, photosynthesis, and leaf and soil energy balances by integrating a range of data streams in MODIS atmospheric and land product with ancillary information. The GLDAS/NOAH (LSM model) is a global, high-resolution, offline (uncoupled to the atmosphere) terrestrial modelling system incorporating ground and satellite observations in order to provide optimal simulations of global land surface states and fluxes in near-real time (Rodell et al. 2004). Finally, the MERRA (Reichle Rolf et al. 2011), a reanalysis dataset, is produced by data assimilation techniques combining observations and modelling results. All the products were resampled to a spatial resolution of 25 km with a temporal resolution of 8 days that extended a period from 2002 to 2010.

2.2.1. *The Combined Optical-Microwave product*

The COM product (Barraza et al. 2015; Barraza et al. 2017) estimates latent heat flux (LE, W m^{-2}, the energy equivalent of ET) using the PM equation driven by satellite-derived global meteorological data and an estimate of surface conductance (G_s) derived from a multi-sensor (COM) model that uses microwave (MI) and optical (VI) satellite data. The model assumes the 8 day microwave indices (MIs) are sensitive to canopy water content and related to surface conductance (G_s), while optical vegetation indices (VIs) are sensitive to leaf chlorophyll concentration and related to G_s. The COM product is generated at a spatial resolution of 25 km and a timestep of 8 days.

2.2.2. *MODIS LE product (MOD16A2)*

The official MODIS LE product (MOD16A2) is based on the PM equation and uses daily meteorological reanalysis data (air temperature, and vapour pressure deficit) and 8 day remotely sensed vegetation structure dynamics (MOD15 LAI product) to estimate G_s and other key environmental drivers (Mu, Zhao, and Running 2011; Mu et al. 2007).

Table 2. Description of the latent heat flux (LE) product used in this study. Where PM is Penman-Monteith.

Product	Land use	Spatial resolution	Temporal resolution	Type	Reference
COM	Regional	25 km	8 days	PM based	Barraza et al. (2017)
MOD16A2	Global	500 m	8 days	PM based	Mu et al. (2007)
BESS	Global	1 km	8 days	Concise process-based model	Jiang and Ryu (2016)
GLDAS/NOAH	Global	25 km	3 h	Numerical product	Marshall et al. (2013)
MERRA/GMA	Global	25 km	3 h	Numerical product	Reichle Rolf et al. (2011)

2.2.3. *Breathing Earth System Simulator*

The BESS is a concise process-based model used to estimate carbon and water fluxes at global scale. The BESS products use MODIS Collection 6 atmosphere products (MOD(Y)D04_L2, MOD(Y)D05_L2, MOD(Y)D06_L2, MOD(Y)D07_L2), and Collection 5 land products (MOD(Y)D11_L2, MCD12Q1, MCD15A2, MCD43B2, MCD43B3), other satellite datasets (e.g. Polarization and Directionality of the Earth's Reflectances, POLDER 3 as in Chen, Menges, and Leblanc 2005), four variables from reanalysis datasets (e.g. Surface Fluxes from NCDEP/NCAR Reanalysis 1 data (Kalnay et al. 1996), and three ancillary datasets as input data (e.g. the Köppen-Geiger global climate classification map (Kottek et al. 2006)). Refer to Jiang and Ryu (2016) for a comprehensive method description.

2.2.4. *Global Land Data Assimilation System (GLDAS/NOAH) model and reanalysis data*

We retrieved the LE product derived from the Global Land Data Assimilation System (GLDAS/NOAH) LSM forced offline (Marshall et al. 2013) and the Modern Era Retrospective-analysis for Research and Applications (MERRA) reanalysis data from coupled LSMs (Schubert, Rood, and Pfaendtner 1993). The GLDAS/NOAH and MERRA product has a 3 h temporal resolution (Rodell et al. 2004).

MERRA (Rienecker et al. 2011), maintained by NASA Global Modelling and Assimilation Office, is the second-generation reanalysis data set, which uses the Goddard Earth Observing System Data Assimilation System-Version 5 (GEOS-5). The GEOS-5 includes GEOS-5 atmospheric circulation model and the grid point statistical interpolation. MERRA implements a procedure called incremental analysis updates (Bloom et al. 1996) to slowly converge modelled calculations towards the observations. A key feature of this global reanalysis is that it takes advantage of a variety of recent satellite observations to improve the estimates of earth's energy and water cycles. The MERRA spans the entire satellite E, from 1979 to the present. Most of the MERRA outputs are archived hourly at its native spatial grid resolution of 2/3° × 1/2°.

2.3. *Seasonal analysis*

Key to understand the vegetation contribution (transpiration) to ET is to relate fluxes to vegetation biophysical parameters. At the DCF we analysed the seasonal cycle of the mean monthly ET as a function of mean monthly precipitation, mean monthly temperature, and LAI. Furthermore, we simulated the monthly effect of surface conductance (G_s) on ET using the PM equation. The G_s is in itself a function of vegetation and environmental variables, including Ta, VPD, soil and leaf water potential, and photosynthetically active radiation; it plays an active role in limiting ET (Allen et al. 1998; Monteith 1985). The objective of this simulation was to understand the possible range of G_s values necessary to obtain the model estimated LE values. For the PM algorithm we used global meteorological data as input from GLDAS/NOAH products with a 3-h temporal resolution (Rodell et al. 2004): air temperature, air pressure, and wind speed. Relative humidity, and roughness lengths for momentum and heat were obtained from the 0.5° × 0.6° (MERRA- GMAO) product (Modern-Era Retrospective Analysis for Research and Applications) (http://disc.sci.gsfc.nasa.gov/daac-bin/FTPSubset.pl) (Schubert, Rood, and Pfaendtner 1993). Meteorological variables were resampled to mean monthly values.

2.4. *Triple collocation*

We used the TC technique developed by Stoffelen ([1998](#)) as a tool to estimate the root mean square error (RMSE) of the LE anomalies generated by GLDAS/NOAH (*X*), COM (*Y*), and MOD16A2 (*Z*). The temporal LE anomalies were defined as the deviations of the original time series from their seasonal climatology:

$$LE_{anomaly} = (LE_{month} - LE_{mean,month})/LE_{std} \tag{1}$$

where $LE_{anomaly}$ is the latent heat flux anomaly (LE), LE_{month} is the monthly LE value, $LE_{mean,\ month}$ is the mean monthly LE value of the time series, and LE_{std} is the standard deviation of LE.

Given these three anomalies dataset, TC is based on selecting a single dataset (*X*) and rescaling the other two (*Y* and *Z*) to this reference via the derivation of specific rescaling factors, as to eliminate systematic differences in their variability. Each observation in these three data sets differs from the hypothetical truth LE anomalies (*t*) based on a linear model as

$$i = \beta_i (t + \varepsilon_i) \tag{2}$$

where β_i and ε_i for $i = x, y, z$ are the TC calibration constants and errors corresponding to GLDAS/NOAH, COM, and MODIS product (MOD16A2), respectively. The following assumptions are required for the TC: (1) zero correlation between errors, which are uncorrelated with each other and with the truth (*t*) and (2) zero error cross-correlation. Then, we set β_x equal to one and estimate the remaining calibration constants via:

$$\hat{\beta}_Y = \frac{Y\ Z}{X\ Z} \tag{3}$$

$$\hat{\beta}_Z = \frac{Y\ Z}{X\ Y} \tag{4}$$

where <> indicates temporal averaging, $\hat{\beta}_Y$ refers to the rescaling factor of product *Y* with respect to *X*, $\hat{\beta}_z$ refers to the rescaling factor of product *Z* with respect to *X*. The variance of the residual errors can be estimated by

$$\sigma_X^2 = \left(X - \frac{Y}{\hat{\beta}_Y}\right)\left(X - \frac{Z}{\hat{\beta}_Z}\right) \tag{5}$$

$$\sigma_Y^2 = \left(\frac{Y}{\hat{\beta}_Y} - X\right)\left(\frac{Y}{\hat{\beta}_Y} - \frac{Z}{\hat{\beta}_Z}\right) \tag{6}$$

$$\sigma_Z^2 = \left(\frac{Z}{\hat{\beta}_Z} - X\right)\left(\frac{Z}{\hat{\beta}_Z} - \frac{Y}{\hat{\beta}_Y}\right) \tag{7}$$

Where <> indicates temporal averaging, σ_X^2, σ_Y^2, and σ_Z^2 are the square-root of the estimated error variances of *X*, *Y*, and *Z* dataset, respectively.

We defined the squareroot of the estimated error variances RMSE as the TC estimates. Since these error variances are anomaly based, the estimates obtained were not

sensitive to the absolute biases of the original time series. However, these error variances are sensitive to the ability of the products to capture individual extreme events (e.g. wet/dry). Since the GLDAS/NOAH was taken as the reference data set, all estimates are given in GLDAS/NOAH climatology. The data chosen as the reference here was the GLDAS LE, since we expect that this product provide benchmark water flux information for the area. To meet the requirement of uncorrelated errors, the products need to be mutually independent (GLDAS/NOAH and the two RS products). However, we acknowledge the possibility that the errors in the different data sets can be cross-correlated, as the used products use the same ancillary data sets, or the similar (imperfect) physics in the RS retrieval algorithms/LSM. We selected this three datasets as the COM is based on passive microwave and optical RS information, the MODIS LE product is solely driven by optical RS data (MOD16A2 and BESS), and the LSM (GLDAS/NOAH) is a more complex model. We applied the TC model to estimate uncertainties over the NATT and DCF sites. We investigated the spatial variability in RMSEs and quantified it using the fractional RMSE (fRMSE) to enhance the differences due to the common signal of the reference standard deviation, where:

$$fRMSE_X = \frac{RMSE_X (X)}{\sigma_{X (X)}} \tag{8}$$

The fRMSE was obtained by presenting the RMSE for data set X ($RMSE_X$) using itself as the reference ($RMSE_{X(X)}$), and then dividing this by the standard deviation of X ($\sigma_{X (X)}$). Across the NATT sites we also calculated fRMSE using LE anomalies from EC measurements and each product.
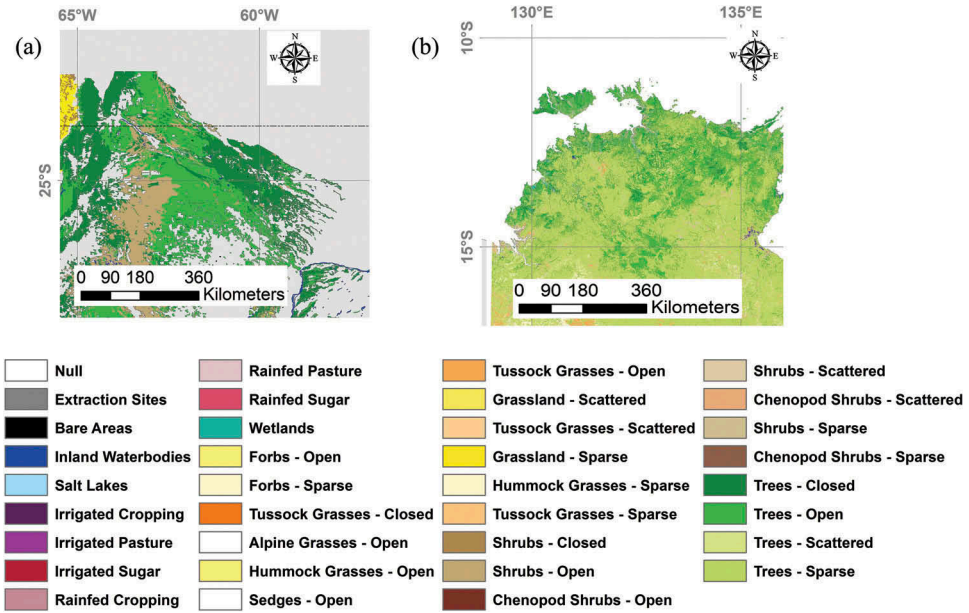
3. Results

3.1. *Comparison of RS (COM, MOD16A2, BESS), LSM, and MERRE LE products*

At the DCF there was not a significant spatial correlation of the average annual LE values within MODIS and COM product (Figure 2). However, GLDAS/NOAH, MERRA, BESS, and MOD16A2 products were not able to capture the spatial heterogeneity expected in the area due to the rainfall and ecosystem gradient. The MOD16A2 and BESS products presented similar spatial pattern (Figure 2).

The COM spatial pattern followed the precipitation and LAI gradient; we found that these variables explained 40 and 30% of the LE model spatial variation ($p < 0.01$), respectively. At the NATT area, the regional observed LE pattern was followed by the COM and MOD16A2 model (Figures 2 and 3). Similarly, the BESS product presented a gradient from north to south but showing lower mean LE values than EC observations. However, LSM (GLDAS/NOAH) and reanalysis dataset (MERRA) did not show the expected gradient. The regional distribution of mean annual LE COM algorithm showed a similar spatial pattern to that of the MOD16A2 (coefficient of determination, $R^2 = 0.72$, and p-value, $p < 0.01$) (Figure 4b). The LE BESS product and the GLDAS/NOAH underestimated LE values. Furthermore, GLDAS/NOAH showed a higher number of pixels with LE values lower than 40 W m^{-2} than the BESS product. Finally, LE MERRA product overestimated LE COM values.

Null	Rainfed Pasture	Tussock Grasses - Open	Shrubs - Scattered
Extraction Sites	Rainfed Sugar	Grassland - Scattered	Chenopod Shrubs - Scattered
Bare Areas	Wetlands	Tussock Grasses - Scattered	Shrubs - Sparse
Inland Waterbodies	Forbs - Open	Grassland - Sparse	Chenopod Shrubs - Sparse
Salt Lakes	Forbs - Sparse	Hummock Grasses - Sparse	Trees - Closed
Irrigated Cropping	Tussock Grasses - Closed	Tussock Grasses - Sparse	Trees - Open
Irrigated Pasture	Alpine Grasses - Open	Shrubs - Closed	Trees - Scattered
Irrigated Sugar	Hummock Grasses - Open	Shrubs - Open	Trees - Sparse
Rainfed Cropping	Sedges - Open	Chenopod Shrubs - Open	

Figure 1. Regression analysis between spatial average annual LE (W m^{-2}) estimated using the combined optical-microwave model (COM) to MOD16A2 BESS, GLDAS/NOAH, and MERRA products at the Dry Chaco forest (DCF). Colorbars represent pixel density.

3.2. *Seasonal analysis at the dry chaco forest*

We observed that all LE products followed the precipitation, LAI, and temperature annual seasonal cycle at the DCF (Figure 5). In general, ET estimates from these products peak in December/March when high surface net radiation drives the seasonal maximum in potential ET. We observed significant differences between the different models monthly LE ($p < 0.001$, degrees of freedom, df = 3, Kruskal Wallis).

The MOD16A2 and MERRA displayed large deviations away from COM, BESS, and GLDAS. The effect of G_s on ET was simulated using the PM equation, meteorological data and high, medium, and low values of G_s (Figure 6). According to simulations, to obtain values as low as the ones presented by the MOD16A2 and BESS products (Figure 6) at DCF the G_s should be less than 1 mm s^{-1}. Furthermore, we evaluated the maximum surface conductance values for DCF estimated using the COM approach and found a range of values between 0–13 mm s^{-1}, with the peak at 8 mm s^{-1}.

3.3. *Certainties in LE products using TC*

We estimated the error between 'true' LE and satellite-derived LE anomalies via the TC method. The MOD16A2 product presented more spatially homogeneous results across Australia, while GLDAS presented a gradient of error across the NATT area (Figure 7a). Larger errors in GLDAS seem to be found in areas of dense vegetation cover Tropical Eucalypt Woodlands (standard error, SE = 8.07%) and Eucalypt woodlands (SE = 20.07%),
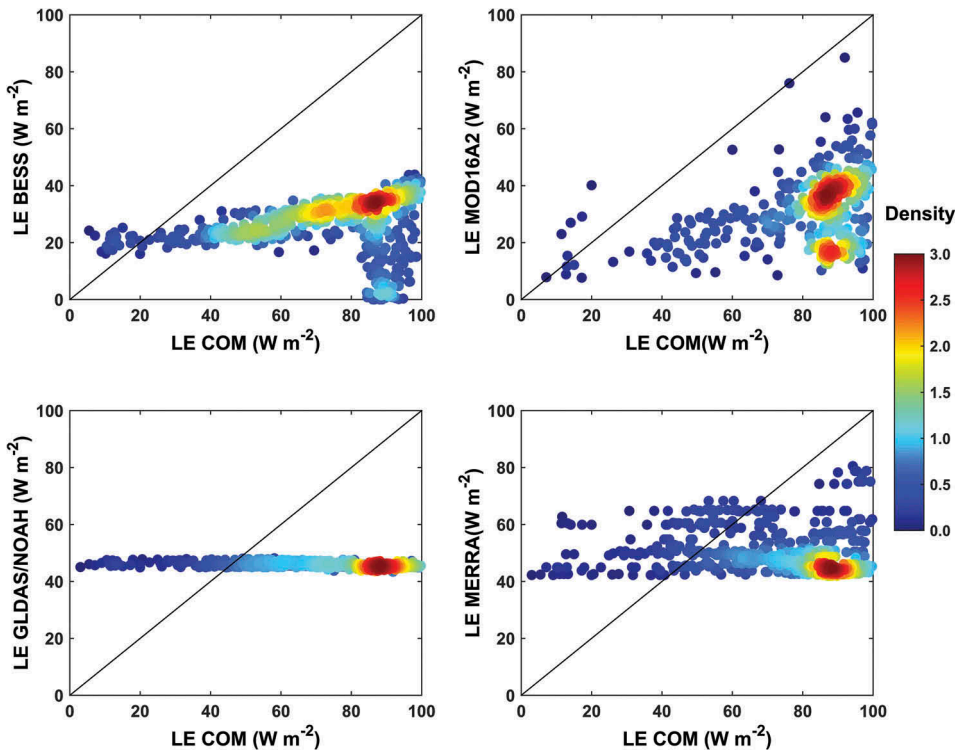
Figure 2. Regression analysis between spatial average annual LE (W m^{-2}) estimated using the combined optical-microwave model (COM) to MOD16A2 BESS, GLDAS/NOAH, and MERRA products at the North Australian tropical transect (NATT). Colorbars represent pixel density.

(Hutley et al. 2011), while COM and MOD16A2 products errors were mainly located in coastal areas.

The spatial pattern of the TC results was commensurable with fRMSE calculated using EC observations, as shown in Figure 7b. Compared to the fRMSE values obtained by the TC method at NATT, we report the highest uncertainties of LE products at the Argentinean Dry Chaco forest (Figure 8). At DCF we observed: (1) the lowest fRMSE for COM and GLDAS LE products, (2) the highest fRMSE was obtained for the MOD16A2 product and, (3) the MOD16A2 product presented more spatially homogeneous results.

4. Discussion and conclusions

In this study, we evaluated the hypothesis that the LE products offer a better performance over areas with EC networks than over sites without *in situ* flux measurements over Southern Hemisphere forest ecosystems. The evaluated products included a LSM, reanalysis, and satellite-derived LE. In general, *in situ* validation has been widely used to analyse the uncertainties of model outputs and to ensure the accuracy of LE product (Barraza et al. 2017; Mu et al. 2007). *In situ* observations provide evidence for local validation; however, there are limitations related to this methodology: (1) error related to spatial extrapolation and (2) ground truth activities are restricted to specific areas, thus
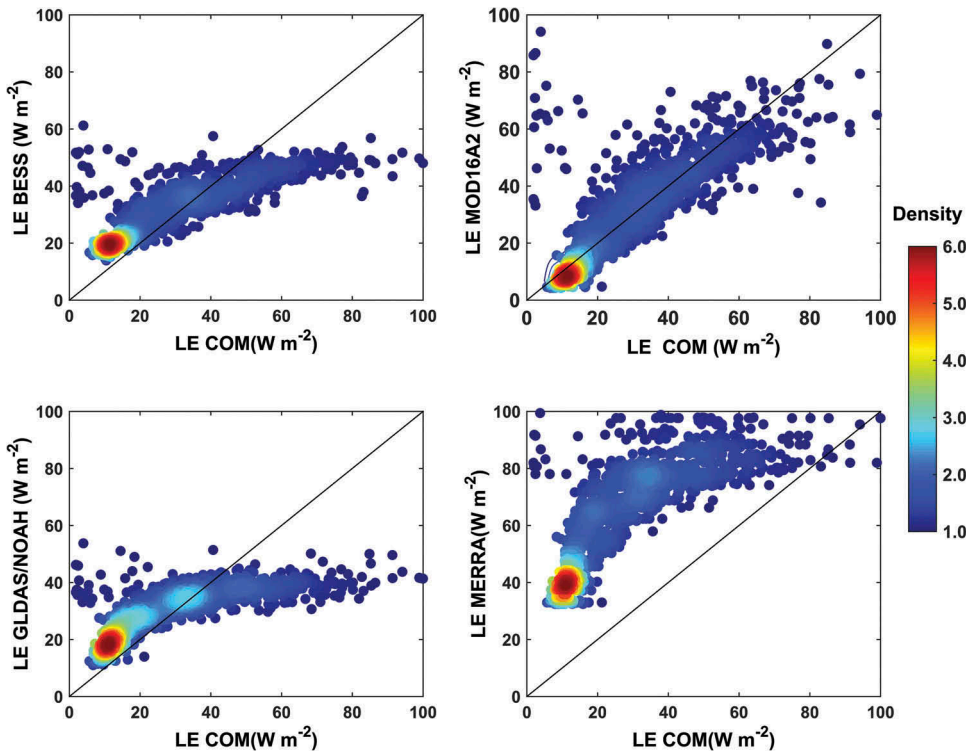
Figure 3. Latitudinal gradient of LE (W m^{-2}) along the NATT from 12° S to 15.5° S. *In situ* eddy covariance method (EC) measurements of LE (W m^{-2}) (dashed blue line), the combined optical-microwave model (COM) (orange dashed line), MOD16A2 (yellow continuous line), GLDAS/NOAH (green line), BESS (purple dashed line), and MERRA (blue line) models.

misses a high percentage of areas where the products are available. To address these limitations we used the TC methodology, because this model provides estimations of spatial uncertainties without the needed of *in situ* flux measurements.

Results show that TC is a robust spatial error estimation of LE at EC sites. The analysis reveals clear spatial patterns over NATT. Furthermore, the spatial pattern of fRMSE was commensurable with the one obtained using EC measurement. In general terms, at this area larger errors in GLDAS/NOAH seemed to be restricted to areas of large biomass, while MOD16A2 and COM errors are mainly located in coastal areas. The last error was probably due to geolocation errors associated with satellite data generation strategy. Notice that bias errors were not detected by a TC analyses, the reason why the GLDAS/NOAH LE showed the lowest fRMSE. However, when we compared EC observations with GLDAS/NOAH estimations we observed a mean bias for GLDAS/NOAH was −30 W m^{-2} for the EC forest sites (see Supplemental material, Table S1). In our previous study (Barraza et al. 2017) we found that the COM and MOD16A2 products presented at the north of the NATT area with a mean RMSE lower than 30 W m^{-2}, with similar spatial patter over these EC sites. We also calculated uncertainties using BESS product (result not shown), as expected based on previous *in situ* validation (see Supplemental material, Table S1) analysis the fRMSE
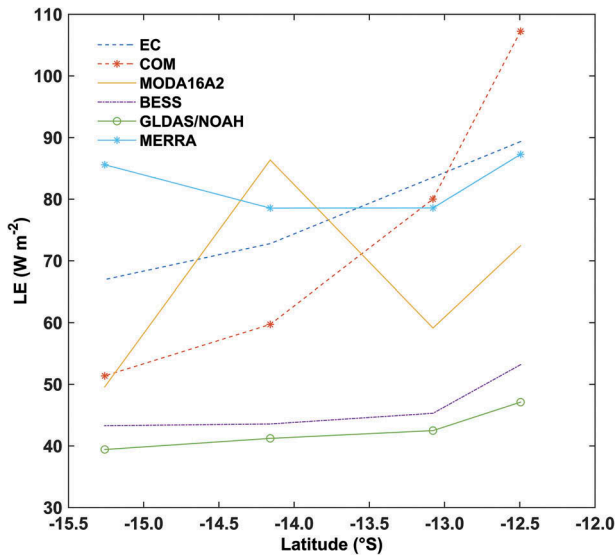
Figure 4. Land cover map of the study areas (*a*) Dry Chaco forest region (DCF), Argentina, and (*b*) North Australian Tropical Transect (NATT), Australia.
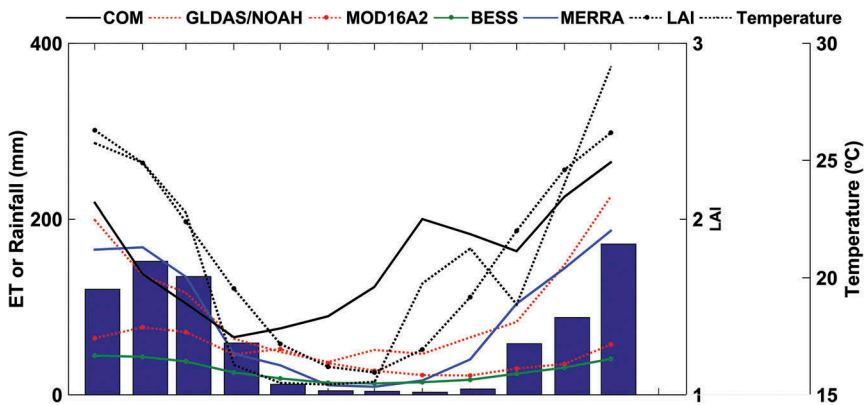

Figure 5. Time series of average monthly evaportranspiration (ET; mm) using the combined optical-microwave model (COM), BESS, MOD16A2, GLDAS/NOAH, and MERRA products, monthly precipitation average for the years 2002 – 2010 (mm) (blue bars), satellite-derived (MODIS) leaf area index (LAI) and atmospheric temperature (*in situ* measurement) at the Dry Chaco forest (DCF).

estimated by TC was close to one. Similarly, Whitley et al. (2016) compared ET estimates derived from six process-based models at the NATT area, and showed that BESS was able to successfully capture the seasonal ET dynamics in this area. Although, we used the most recent version of BESS product with updated MODIS LAI product (version 6), the model underestimated LE when compared to EC measurements.

Moreover, the TC model provides evidence of the uncertainties over the DCF where no LE measurement was available. Based on the TC result at the DCF, the COM and GLDAS/NOAH LE products presented the best performance (lower fRMSE than MODIS
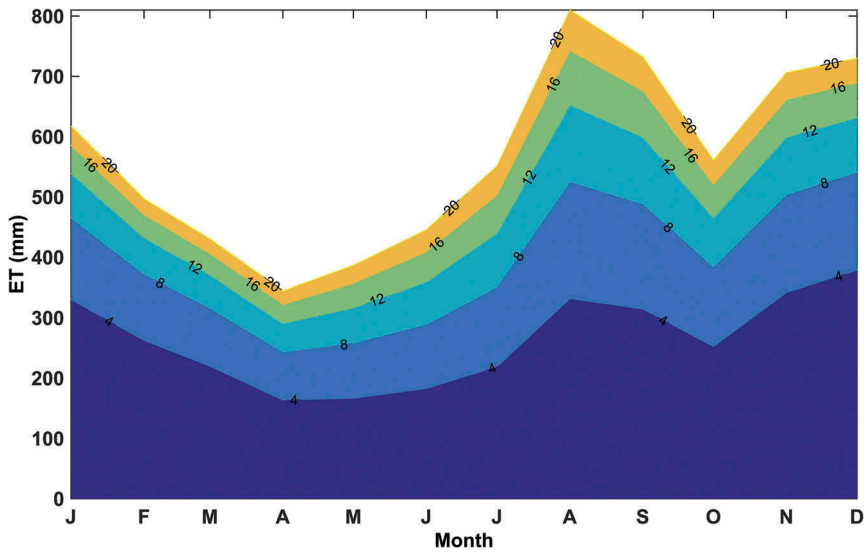
Figure 6. Montly evapotranspiration (ET; mm) simulated time series as a function of canopy conductance (G_s; mm s^{-1}) using the Penman-Monteith equation and meteorological data at the Dry Chaco forest (DCF). Color scale, from blue to white, represent G_s values from <4 to >20 mm s^{-1} with the number above the contour line.
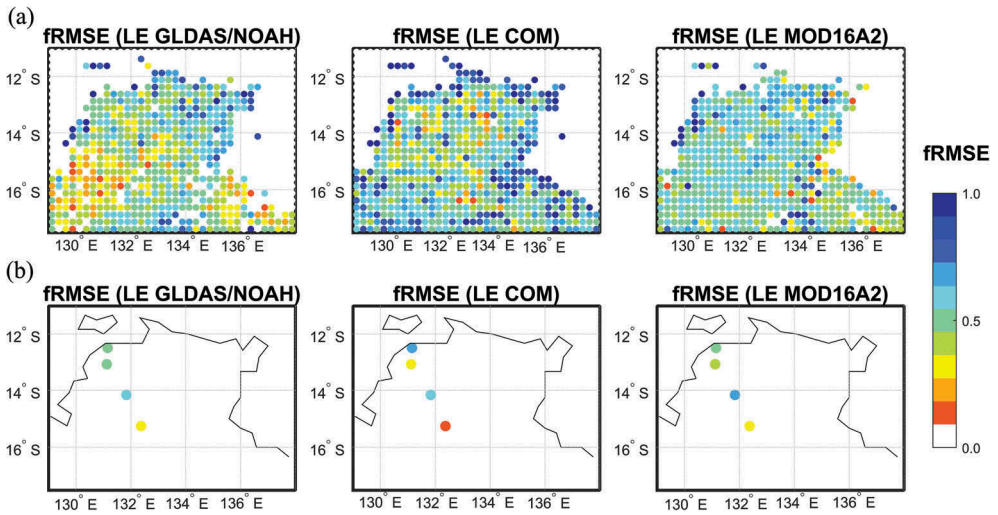
Figure 7. Maps of fRMSE estimated from (*a*) triple collocation (upper row) and from (*b*) eddy covariance measurements (EC) (lower row); for GLDAS/NOAH, combined optical-microwave model (COM) and MODIS (MOD16A2) product at the North Australian tropical transect (NATT). From North to South the EC sites are AU-Hsp. AU-Ade, AU-DaS, and AU-Dry.

product). Compared to NATT results, the TC shows that MOD16A2 product presented the highest fRMSE at DCF. Lowest errors were observed for the regional RS product (COM) in comparison to MOD16A2 LE. Furthermore, the seasonal analysis showed that the COM, GLDAS/NOAH, and MERRA models show higher mean monthly LE values for
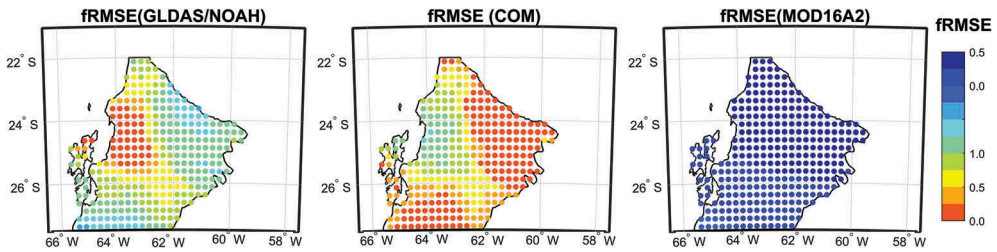
Figure 8. Maps of fRMSE estimated from triple collocation for GLDAS/NOAH, combined optical-microwave model (COM), and MODIS (MOD16A2) product at the Dry Chaco forest (DCF).

this forest, at times ET estimations were higher than precipitation. Several studies provide evidence that the dominated vegetation over Chaco Forest (*Schinopsis lorentzii*, *Aspidosperma quebracho-blanco*, *Prosopis alba*, *Prosopis nigra*) extract water and nutrients from much greater soil depths (Jobbágy et al. 2008). MODIS and BESS ET product presented monthly average ET values lower than mean monthly precipitation. However, several studies show that MODIS ET product underestimated ET over areas with water-limited ecosystems (Ramoelo et al. 2014). The overestimation of MODIS LAI absolute values and seasonal amplitude will drive errors in the MODIS ET product. A simulation analysis based on the PM equation showed that to estimate ET values as lowest as the ones obtained by MOD16A2 and BESS product, the mean surface conductance should be 1 mm s^{-1}. At regional scale, the maximum G_s estimated using the COM model values was between 0–13 mm s^{-1} with the peak at 8 mm s^{-1} which were similar to the ones reported by the literature for Deciduous Forest and Savanna (Kelliher et al. 1995; Barraza et al. 2015; Rodrigues et al. 2014).

Despite differences between RS, LSM, and reanalysis LE products (e.g. algorithms and inputs, among others), TC results suggested that the LE products performed better over areas within EC networks (FLUXNET, Ameriflux, OzFlux). Thus, GLDAS is a data-driven model that used less than ideal observational data to be assimilated in the model, most likely lowering the performance over areas like DCF. The LSM used the MODIS Land Cover product which incorrectly classified DCF as both Deciduous Broadleaf Forest and as grassland. Furthermore, MOD16 and BESS model are driven by other MODIS data products (LAI, Land Cover, and Albedo). The global MODIS LAI and Land Cover products have not been validated in the DCF. Over this area, the backup algorithm to estimate LAI is based on LAI vs. NDVI relationship, introducing error in the LE algorithm. At the NATT area, the MODIS LAI product gave reasonable estimates for LAI for most cover and land use types, based on previous analysis over Australia (Hill et al. 2006). However, Hill et al. (2006) also identified misclassifications of the MODIS Land Cover product over Australia. By contrast, the COM model does not use MODIS LAI nor Land Cover products. The COM is a regional model driven by meteorological forcing data (GMAO- MERRA reanalysis dataset and GLDAS/NOAH) and optical and MIs. Thus as, COM uses a semi-empirical model based on G_s- RS index regressions that require local validation. Finally, MERRA reanalysis data resulted in the lowest performance over the two study sites (NATT and DCF). This model assimilates numerous satellite data streams (precipitation, wind speed, radiosonde, station, aircraft, ship, and others) using the GEOS-5 data assimilation system (Reichle Rolf et al. 2011). The quality of the input dataset is especially important to the reanalysis land

surface scheme in order to derive accurate water and energy fluxes involving a land data assimilation, which will profoundly affect the resulting LE estimates.

The existing biases between the LE estimates over areas without ground-based measurement arise from the following major causes: (1) uncertainties in others vegetation inputs used in each model, like LAI and land cover, and (2) uncertainties in meteorological inputs. *In situ* EC towers are more likely placed within homogeneous areas in which vegetation cover, type, and structural parameters are better characterized than adjacent areas which may be more heterogeneous and non-conforming to existing land cover characterization schemes. This could partly explain why well-instrumented *in situ* measurement sites may have resulted in better-LE estimates compared with non-instrumented sites. Performance of the LE algorithms could be largely improved when *in situ* meteorological measurements (Mu, Zhao, and Running 2011) and with a better vegetation characterized are used; however, direct measurement of LE in the field is expensive and difficult. Results from our inter-comparison study between available LE models would guide future studies providing evidence about LE uncertainties over areas with and without ground-based measurements.

Acknowledgements

Disclosure statement

Funding

References

Allen, R. G., L. S. Pereira, D. Raes, and M. Smith; others. 1998. "Crop Evapotranspiration-Guidelines for Computing Crop Water Requirements-FAO Irrigation and Drainage Paper 56." *FAO, Rome* 300: 6541.

Baldocchi, D. D., B. B. Hincks, and T. P. Meyers. 1988. "Measuring Biosphere-Atmosphere Exchanges of Biologically Related Gases with Micrometeorological Methods." *Ecology* 69 (5): 1331–1340. doi:10.2307/1941631.

Barraza, V., N. Restrepo-Coupe, A. Huete, F. Grings, and E. Van Gorsel. 2015. "Passive Microwave and Optical Index Approaches for Estimating Surface Conductance and Evapotranspiration in Forest Ecosystems." *Agricultural and Forest Meteorology* 213 (November): 126–137. doi:10.1016/j.agrformet.2015.06.020.

Barraza, V., N. Restrepo-Coupe, A. Huete, F. Grings, J. Beringer, J. Cleverly, and D. Eamus. 2017. "Estimation of Latent Heat Flux over Savannah Vegetation across the North Australian Tropical Transect from Multiple Sensors and Global Meteorological Data." *Agricultural and Forest Meteorology* 232 (January): 689–703. doi: 10.1016/j.agrformet.2016.10.013.

Bloom, C. S., L. L. Takacs, A. Da Silva, and D. Ledvina. 1996. "Data Assimilation Using Incremental Analysis Updates." *Monthly Weather Review* 124 (June). doi:10.1175/1520-0493(1996)124<1256: DAUIAU>2.0.CO;2.

Chen, J. M., C. H. Menges, and S. G. Leblanc. 2005. "Global Mapping of Foliage Clumping Index Using Multi-Angular Satellite Data." *Remote Sensing of Environment* 97 (4): 447–457. doi:10.1016/j.rse.2005.05.003.

Ek, M. B. 2003. "Implementation of Noah Land Surface Model Advances in the National Centers for Environmental Prediction Operational Mesoscale Eta Model." *Journal of Geophysical Research* 108 (D22): 8851. doi:10.1029/2002JD003296.

Fang, H. W. Shanshan, J. Chongya, and S. Klaus. 2012. "Theoretical Uncertainty Dataset of Global MODIS, CYCLOPES, and GLOBCARBON leaf area index (LAI) Generated from a Triple Collocation Error Model (TCEM)." PANGAEA Documentation. EPIC3Bremerhaven, PANGAEA. http://epic.awi.de/31314/

Gasparri, N. I., and G. Baldi. 2013. "Regional Patterns and Controls of Biomass in Semiarid Woodlands: Lessons from the Northern Argentina Dry Chaco." *Regional Environmental Change* 13 (6): 1131–1144. doi:10.1007/s10113-013-0422-x.

Gasparri, N. I., and H. R. Grau. 2009. "Deforestation and Fragmentation of Chaco Dry Forest in NW Argentina (1972–2007)." *Forest Ecology and Management* 258 (6): 913–921. doi: 10.1016/j.foreco.2009.02.024.

Hill, M. J., U. Senarath, A. Lee, M. Zeppel, J. M. Nightingale, Richard (Dick) J. Williams, and T. R. McVicar. 2006. "Assessment of the MODIS LAI Product for Australian Ecosystems." *Remote Sensing of Environment* 101 (4): 495–518. doi:10.1016/j.rse.2006.01.010.

Hutley, L. B., J. Beringer, P. R. Isaac, J. M. Hacker, and L. A. Cernusak. 2011. "A Sub-Continental Scale Living Laboratory: Spatial Patterns of Savanna Vegetation over a Rainfall Gradient in Northern Australia." *Agricultural and Forest Meteorology* 151 (11): 1417–1428. doi:10.1016/j.agrformet.2011.03.002.

Jiang, C., and Y. Ryu. 2016. "Multi-Scale Evaluation of Global Gross Primary Productivity and Evapotranspiration Products Derived from Breathing Earth System Simulator (BESS)." *Remote Sensing of Environment* 186 (December): 528–547. doi:10.1016/j.rse.2016.08.030.

Jobbágy, E. G., M. D. Nosetto, C. S. Santoni, and G. Baldi. 2008. "El Desafío Ecohidrológico De Las Transiciones Entre Sistemas Leñosos Y Herbáceos En La Llanura Chaco-Pampeana." *Ecología Austral* 18 (3): 305–322.

Kalnay, E., M. Kanamitsu, R. Kistler, W. Collins, D. Deaven, L. Gandin, M. Iredell, et al. 1996. "The NCEP/NCAR 40-Year Reanalysis Project." *Bulletin of the American Meteorological Society* 77 (3): 437–471. doi:10.1175/1520-0477(1996)077<0437:TNYRP>2.0.CO;2.

Kelliher, F. M., R. Leuning, M. R. Raupach, and E.-D. Schulze. 1995. "Maximum Conductances for Evaporation from Global Vegetation Types." *Agricultural and Forest Meteorology* 73 (1–2): 1–16. doi:10.1016/0168-1923(94)02178-M.

Koch, G. W., P. M. Vitousek, W. L. Steffen, and B. H. Walker. 1995. "Terrestrial Transects for Global Change Research." *Vegetatio* 121 (1–2): 53–65. doi:10.1007/BF00044672.

Kottek, M., J. Grieser, C. Beck, B. Rudolf, and F. Rubel. 2006. "World Map of the Köppen-Geiger Climate Classification Updated." *Meteorologische Zeitschrift* July: 259–263. doi:10.1127/0941-2948/2006/0130.

Marshall, M., K. Tu, C. Funk, J. Michaelsen, P. Williams, C. Williams, J. Ardö, et al. 2013. "Improving Operational Land Surface Model Canopy Evapotranspiration in Africa Using a Direct Remote Sensing Approach." *Hydrology Earth Systems Sciences* 17 (3): 1079–1091. doi:10.5194/hess-17-1079-2013.

Monteith, J. L. 1985. "Evaporation from Land Surfaces: Progress in Analysis and Prediction since 1948." In *Advances in Evapotranspiration*, 4–12. Chicago, ILL: ASAE, St. Joseph, Michigan.

Mu, Q., F. A. Heinsch, M. Zhao, and S. W. Running. 2007. "Development of a Global Evapotranspiration Algorithm Based on Modis and Global Meteorology Data." *Remote Sensing of Environment* 111: 519–536. doi: 10.1016/j.rse.2007.04.015.

Mu, Q., M. Zhao, and S. W. Running. 2011. "Improvements to a MODIS Global Terrestrial Evapotranspiration Algorithm." *Remote Sensing of Environment* 115 (8): 1781–1800. doi:10.1016/j.rse.2011.02.019.

Ramoelo, A., N. Majozi, R. Mathieu, N. Jovanovic, A. Nickless, and S. Dzikiti. 2014. "Validation of Global Evapotranspiration Product (MOD16) Using Flux Tower Data in the African Savanna, South Africa." *Remote Sensing* 6 (8): 7406–7423. doi:10.3390/rs6087406.

Reichle Rolf, H., R. D. Koster, G. J. M. De Lannoy, B. A. Forman, Q. Liu, S. P. P. Mahanama, and A. Touré. 2011. "Assessment and Enhancement of MERRA Land Surface Hydrology Estimates." *Journal of Climate* 24 (24): 6322–6338. doi:10.1175/JCLI-D-10-05033.1.

Restrepo-Coupe, N., A. Huete, K. Davies, J. Cleverly, J. Beringer, D. Eamus, E. Van Gorsel, L. B. Hutley, and W. S. Meyer. 2015. "MODIS Vegetation Products as Proxies of Photosynthetic Potential: A Look across Meteorological and Biologic Driven Ecosystem Productivity." *Biogeosciences Discussions* 12 (23): 19213–19267. doi:10.5194/bgd-12-19213-2015.

Rienecker, M. M., M. J. Suarez, R. Gelaro, R. Todling, J. Bacmeister, E. Liu, M.G. Bosilovich, S. D. Schubert, L. Takacs, G.-K. Kim, S. Bloom, J. Chen, D. Collins, A. Conaty, A. da Silva, W. Gu, J. Joiner, R. D. Koster, R. Lucchesi, A. Molod, T. Owens, S. Pawson, P. Pegion, C. R. Redder, R. Reichle, F. R. Robertson, A. G. Ruddick, M. Sienkiewicz, and J. Woollen. 2011. "MERRA: NASA's Modern-era Retrospective Analysis for Research and Applications." *Journal of Climate* 24 (14): 3624–3648. doi:10.1175/JCLI-D-11-00015.1.

Rodell, M., J. S. Famiglietti, J. Chen, S. I. Seneviratne, P. Viterbo, S. Holl, and C. R. Wilson. 2004. "Basin Scale Estimates of Evapotranspiration Using GRACE and Other Observations." *Geophysical Research Letters* 31 (20). http://onlinelibrary.wiley.com/doi/10.1029/2004GL020873/full.

Rodrigues, T. R., G. L. Vourlitis, F. D. A. Lobo, R. G. de Oliveira, and J. D. S. Nogueira. 2014. "Seasonal Variation in Energy Balance and Canopy Conductance for a Tropical Savanna Ecosystem of South Central Mato Grosso, Brazil." *Journal of Geophysical Research: Biogeosciences* 119 (1): 2013JG002472. doi:10.1002/2013JG002472.

Rosero, E., Z.-L. Yang, L. Gulden, G.-Y. Niu, and D. J. Gochis. 2009. "Evaluating Enhanced Hydrological Representations in Noah LSM over Transition Zones: Implications for Model Development." *Journal of Hydrometeorology* 10 (3): 600–622. doi:10.1175/2009JHM1029.1.

Schubert, S. D., R. B. Rood, and J. Pfaendtner. 1993. "An Assimilated Dataset for Earth Science Applications." *Bulletin of the American Meteorological Society* 74 (12): 2331–2342. doi:10.1175/1520-0477(1993)074<2331:AADFES>2.0.CO;2.

Sea, W. B., P. Choler, J. Beringer, R. A. Weinmann, L. B. Hutley, and R. Leuning. 2011. "Documenting Improvement in Leaf Area Index Estimates from Modis Using Hemispherical Photos for Australian Savannas." *Agricultural and Forest Meteorology* 151 (11): 1453–1461. doi:10.1016/j.agrformet.2010.12.006.

Stoffelen, A. 1998. "Toward the True Near-Surface Wind Speed: Error Modeling and Calibration Using Triple Collocation." *Journal of Geophysical Research: Oceans* 103 (C4): 7755–7766. doi:10.1029/97JC03180.

Trenberth, K. E., J. T. Fasullo, and J. Kiehl. 2009. "Earth's Global Energy Budget." *Bulletin of the American Meteorological Society* 90 (3): 311–323. doi:10.1175/2008BAMS2634.1.

Whitley, R., J. Beringer, L. B. Hutley, G. Abramowitz, M. G. De Kauwe, R. Duursma, B. Evans, et al. 2016. "A Model Inter-Comparison Study to Examine Limiting Factors in Modelling Australian Tropical Savannas." *Biogeosciences* 13 (11): 3245–3265. doi:10.5194/bg-13-3245-2016.

Yilmaz, M. T., and W. T. Crow. 2014. "Evaluation of Assumptions in Soil Moisture Triple Collocation Analysis." *Journal of Hydrometeorology*. http://agris.fao.org/agris-search/search.do?recordID=US201500059966.